ISSN 1392–1320 MATERIALS SCIENCE (MEDŽIAGOTYRA). Vol. 23, No. 1. 2017

Characterization of Hydrogen-Storage Properties and Physical Properties of Zinc Borohydride and Transition Metals-Added Magnesium Hydride

Young Jun KWAK [1], Hye Ryoung PARK [2], Myoung Youp SONG [3] *

[1] *Department of Materials Engineering, Graduate School, Chonbuk National University, 567 Baekje-daero Deokjin-gu Jeonju, 54896, Republic of Korea*
[2] *School of Applied Chemical Engineering, Chonnam National University, 77 Yongbong-ro Buk-gu Gwangju, 61186, South Korea*
[3] *Division of Advanced Materials Engineering, Research Center of Advanced Materials Development, Engineering Research Institute, Chonbuk National University, 567 Baekje-daero Deokjin-gu Jeonju, 54896, Republic of Korea*

crossref http://dx.doi.org/10.5755/j01.ms.23.1.14878

Received 29 April 2016; accepted 2 September 2016

In this work, 90 wt.% MgH_2+5 wt.% Ni+1.7 wt.% $Zn(BH_4)_2$+1.7 wt.% Ti+1.7 wt.% Fe samples (named 90MgH_2+5Ni+ +1.7$Zn(BH_4)_2$+1.7Ti+1.7Fe) were prepared by milling in a planetary ball mill in a hydrogen atmosphere. The fraction of additives was small (10 wt.%) in order to increase hydriding and dehydriding rates without decreasing the hydrogen storage capacity much. The hydrogen absorption and release properties of the prepared samples were investigated. 90MgH_2+5Ni+1.7$Zn(BH_4)_2$+1.7Ti+1.7Fe had an effective hydrogen storage capacity of 5 wt.%. The activation of 90MgH_2+5Ni+1.7$Zn(BH_4)_2$+1.7Ti+1.7Fe was completed after 2 hydriding-dehydriding cycles. At $n = 3$, the sample absorbed 4.14 wt.% H for 5 min and 5.00 wt.% H for 60 min at 593 K under 12 bar H_2. The sample dehydrided at the 3rd hydriding-dehydriding cycle contained Mg and small amounts of β-MgH_2, MgO, Mg_2Ni, $TiH_{1.924}$, and Fe. The BET specific surface areas of the sample after milling in a hydrogen atmosphere and after 3 hydriding-dehydriding cycles were 57.9 and 53.2 m^2/g, respectively.

Keywords: hydrogen absorbing materials, ball milling, scanning electron microscopy (SEM), X-ray diffraction, Ni, $Zn(BH_4)_2$, Fe, and Ti-added MgH_2-based alloy.

1. INTRODUCTION

Magnesium hydride, which draws attention as a hydrogen storage material, has high gravimetric hydrogen density and is inexpensive and abundant in the earth's crust [1]. However, its reaction rates with hydrogen are very low. Many researchers tried to increase the hydriding and dehydriding rates of magnesium [2 – 4] by alloying certain metals [5 – 9] with it and synthesizing compounds such as $CeMg_{12}$ [10].

Many researches [11 – 20] were performed on metal borohydrides [$M(BH_4)_n$] as promising candidates for advanced hydrogen storage materials due to their high specific volumetric hydrogen-storage capacities. The complex metal hydride $Zn(BH_4)_2$ has also drawn attention due to its high specific volumetric hydrogen-storage capacity (8.4 wt.%) [21 – 24] and low decomposition temperature (323 – 393 K).

Bobet et al. [8] reported that mechanical grinding in H_2 of magnesium powder converted Mg to MgH_2 partially. Its conversion ratio could be improved by increasing the milling time or by adding a 3d-element. Shahi et al. [25] mechanically milled MgH_2 with transition metals (Ti, Fe, and Ni). They reported that the decomposition temperature of MgH_2 was reduced and the rehydrogenation kinetics was correspondingly enhanced.

In the present work, $Zn(BH_4)_2$, Ni, Ti, and Fe were selected to be added in order to improve the hydriding and dehydriding rates of magnesium. In our previous works [26], a $Zn(BH_4)_2$ sample was prepared by milling $ZnCl_2$ and $NaBH_4$ in a planetary ball mill in an Ar atmosphere. A simultaneous addition of $Zn(BH_4)_2$, Ni, Ti, and Fe is expected to lead to refining of MgH_2 particles since brittle $Zn(BH_4)_2$ and hard Ni, Fe, and Ti particles will help the MgH_2 particles be milled with effect. Ni is known to form Mg_2NiH_4, which has higher hydriding and dehydriding rates than magnesium [27]. A relatively large percentage (5 wt.%) of Ni was added to increase the dehydriding rate of MgH_2. Small percentages of $Zn(BH_4)_2$, Ti, and Fe were added not to decrease the fraction of MgH_2 too much so that the prepared sample may have a large hydrogen-storage capacity.

90wt.% MgH2+5wt.% Ni+1.7wt.% Zn(BH4)2+1.7wt.% Ti+ +1.7 wt.% Fe samples (named 90MgH_2+5Ni+1.7$Zn(BH_4)_2$+ +1.7Ti+1.7Fe) were prepared by milling in a planetary ball mill in a hydrogen atmosphere. The fraction of additives was small (10 wt.%) in order to increase hydriding and dehydriding rates without decreasing the hydrogen storage capacity significantly. The hydrogen absorption and release properties of the prepared samples were investigated. In addition, the physical properties, such as microstructure, particle size distribution, and BET (Brunauer-Emmett-Teller) specific surface area, of the samples after milling in hydrogen and after hydriding-dehydriding cycling were examined.

*Corresponding author. Tel.: +82-63-270-2379; fax: +82-63-270-2386.
E-mail address: *songmy@jbnu.ac.kr* (M.Y. Song)

2. EXPERIMENTAL DETAILS

The starting materials were MgH_2 (Magnesium hydride, Aldrich, hydrogen-storage grade), Ni (Nickel powder, Alfa Aesar, average particle size 2.2 – 3.0 μm, 99.9 % (metals basis), C typically < 0.1), Ti (Titanium powder, Aldrich, – 325 mesh (– 0.044 mm), 99 % (metals basis)), Fe (Alfa Aesar GmbH (Germany), Iron particle size < 10 μm, purity 99.9 %), and $Zn(BH_4)_2$ prepared in our previous works [26].

Milling in hydrogen of a mixture with a composition of 90 wt.% MgH_2+5 wt.% Ni+1.7 wt.% $Zn(BH_4)_2$+ 1.7 wt.% Ti+ +1.7 wt.% Fe (total weight = 8 g) was performed in a planetary ball mill (Planetary Mono Mill; Pulverisette 6, Fritsch), which has a hermetically-sealed stainless steel container (with 105 hardened steel balls, total weight = 360 g). The sample to ball weight ratio was 1:45. Samples were handled in a glove box under Ar to prevent oxidation. The disc revolution speed was 400 rpm. The mill container (volume of 250 ml) was filled with high purity hydrogen gas (≈ 12 bar). Milling in hydrogen was performed for 2 h [28].

The variations, with time, of the quantities of hydrogen absorbed and released by the prepared samples were measured under the hydrogen pressures maintained nearly constant, using a Sievert's type hydriding and dehydriding apparatus, as described previously [29]. X-ray diffraction (XRD) patterns for the prepared samples were obtained using a Rigaku D/MAX 2500 powder diffractometer with Cu Kα radiation (diffraction angle range 10 – 80°, scan speed 4°/min). The microstructures of the samples after milling in hydrogen and after hydriding-dehydriding cycling were observed using a scanning electron microscope (SEM, JEOL JSM-6400) operated at 20 kV. Particle size distributions and BET specific surface areas of the samples were analyzed using UPA-150 (Microtrac, USA) and ASAP2010 (Micrometrics, USA), respectively.

3. RESULTS

Fig. 1 shows the SEM micrographs of $90MgH_2$+5Ni+1.7$Zn(BH_4)_2$+1.7Ti+1.7Fe after milling in a hydrogen atmosphere. The particle size of the sample is not homogeneous. The sample has small particles, large particles, and agglomerates. The surfaces of some agglomerates are quite flat. Milling in hydrogen of MgH_2 with Ni, $Zn(BH_4)_2$, Ti, and Fe is considered to create defects on the surface and in the inside of MgH_2 particles, to produce reactive clean surfaces, and to reduce the particle size of MgH_2.

The XRD pattern of $90MgH_2$+5Ni+1.7$Zn(BH_4)_2$+ +1.7Ti+1.7Fe after milling in hydrogen is shown in Fig. 2. The sample contains β-MgH_2, γ-MgH_2, Ni, Ti, Fe, and MgO. β-MgH_2, having a tetragonal structure, is a low pressure form of MgH_2. γ-MgH_2, having an orthorhombic structure, is one of the high pressure forms of MgH_2. This shows that γ-MgH_2 is formed during milling in a hydrogen atmosphere even under the low hydrogen pressure of about 12 bar. A small amount of MgO is formed. In this XRD pattern, the background is quite high and the peaks are broad, demonstrating the slightly noncrystalline nature of the sample after milling in hydrogen. The phases related to $Zn(BH_4)_2$ are not detected. This is believed to be since the small quantity of $Zn(BH_4)_2$ is contained in the sample and they may appear at the diffraction angles similar to those of other phases. The quite high back ground also makes difficult the appearance of weak diffraction lines.

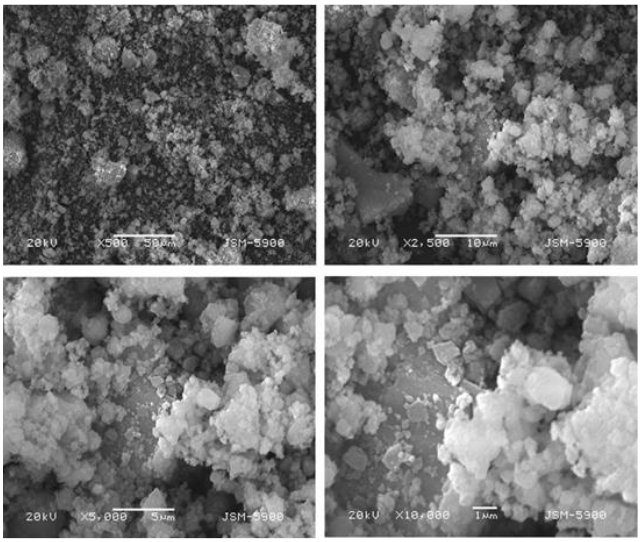

Fig. 1. SEM micrographs of $90MgH_2$+5Ni+1.7$Zn(BH_4)_2$+ +1.7Ti+1.7Fe after milling in hydrogen

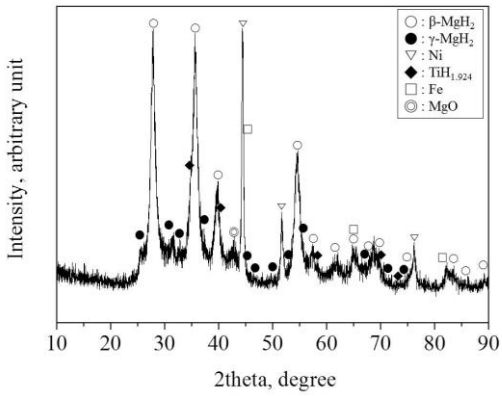

Fig. 2. XRD pattern of $90MgH_2$+5Ni+1.7$Zn(BH_4)_2$+1.7Ti+1.7Fe after milling in hydrogen

The percentage of absorbed hydrogen, H_a, is expressed with respect to sample weight. Fig. 3 shows the variation of the H_a vs. t curve and the log H_a vs. t curve of $90MgH_2$ + 5Ni + 1.7$Zn(BH_4)_2$ + 1.7Ti + 1.7Fe at 593 K under 12 bar H_2 with the number of cycles, n. From n = 1, the initial hydriding rate is very high, and becomes low after about 10 min. As the number of cycles increases from 1 to 3, the initial hydriding rate increases. The quantity of hydrogen absorbed for 60 min, H_a(60 min), increases from n = 1 to n = 2 and decreases from n = 2 to n = 3. At n = 1, the sample absorbs 3.82 wt.% H for 5 min and 4.93 wt.% H for 60 min. At n = 3, the sample absorbs 4.14 wt.% H for 5 min and 5.00 wt.% H for 60 min. The log H_a vs. t curve enables us to distinguish data points clearly. Fig. 3 b shows plainly that the initial hydriding rate increses as the number of cycles increases. Table 1 presents the variation of the absorbed hydrogen quantity with time for $90MgH_2$ + 5Ni + 1.7$Zn(BH_4)_2$ + 1.7Ti + 1.7Fe at 593 K under 12 bar H_2 at n = 1 – 3.

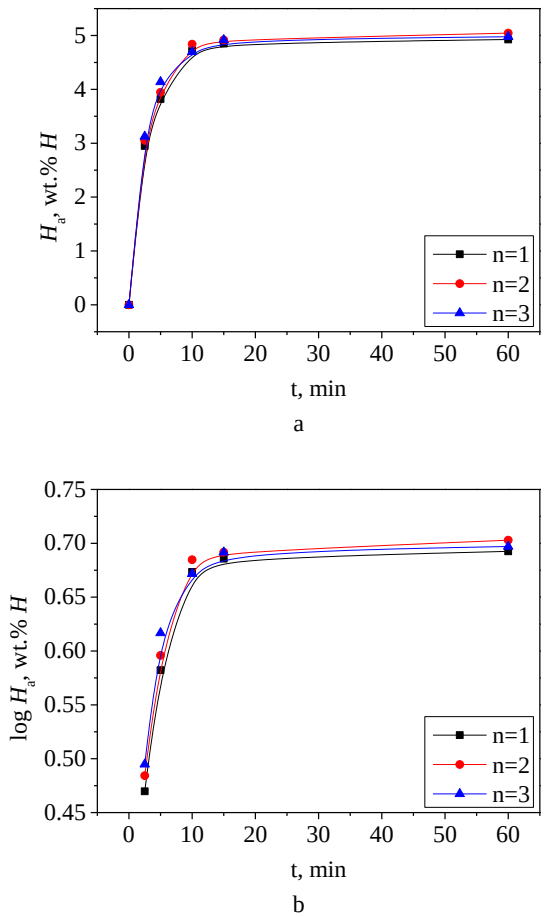

Fig. 3. Variations of (a) the H_a vs. t curve and (b) the log H_a vs. t curve of $90MgH_2 + 5Ni + 1.7\ Zn(BH_4)_2 + 1.7Ti + 1.7Fe$ at 593 K under 12 bar H_2 with the number of cycles, n

Table 1. Variation of the absorbed hydrogen quantity with time for $90MgH_2$+5Ni+1.7$Zn(BH_4)_2$+1.7Ti+1.7Fe at 593 K under 12 bar H_2 at $n = 1 – 3$

Absorbed hydrogen quantity (wt.% H)					
	2.5 min	5 min	10 min	15 min	60 min
$n = 1$	2.95	3.82	4.71	4.85	4.93
$n = 2$	3.05	3.94	4.84	4.92	5.05
$n = 3$	3.13	4.14	4.70	4.92	5.00

The percentage of desorbed hydrogen, H_d, is also expressed with respect to the sample weight. The variation of the H_d vs. t curve of $90MgH_2 + 5Ni + 1.7Zn(BH_4)_2$+ + 1.7Ti + 1.7Fe at 593 K under 1.0 bar H_2 with the number of cycles, n, is shown in Fig. 4. The initial dehydriding rate is quite high, and becomes low after about 40 min. At $n = 2$ and $n = 3$, the initial dehydriding rate is higher and the quantity of hydrogen desorbed for 60 min is larger than those at $n = 1$. At $n = 2$ and $n = 3$, the initial dehydriding rate and the quantity of hydrogen desorbed for 60 min are nearly similar. At $n = 1$, the sample desorbs 1.46 wt.% H for 10 min and 4.57 wt.% H for 60 min. At $n = 3$, the sample desorbs 1.77 wt.% H for 10 min and 4.67 wt.% H for 60 min. Table 2 presents the variation of the desorbed hydrogen quantity with time for $90MgH_2$+5Ni+1.7$Zn(BH_4)_2$+1.7Ti+1.7Fe at 593 K under 1.0 bar H_2 at $n = 1$ and $n = 3$.

Fig. 3 and Fig. 4 show that the activation of $90MgH_2$+ +5Ni+1.7$Zn(BH_4)_2$+1.7Ti+1.7Fe is completed after 2 hydriding-dehydriding cycles.

Fig. 5 shows the SEM micrographs of $90MgH_2 + 5Ni$+ +1.7$Zn(BH_4)_2$+1.7Ti+1.7Fe dehydrided at the 3rd hydriding-dehydriding cycle. The particle size of the sample is not homogeneous. The sample has small particles, large particles, and agglomerates. The surfaces of some agglomerates are rounded. Particles got rounded and slightly larger, compared with those after milling in hydrogen.

Table 2. Variation of the desorbed hydrogen quantity with time for $90MgH_2 + 5Ni + 1.7Zn(BH_4)_2 + 1.7Ti + 1.7Fe$ at 593 K under 1.0 bar H_2 at $n = 1$ and $n = 3$

Desorbed hydrogen quantity (wt.% H)					
	5 min	10 min	20 min	30 min	60 min
$n = 1$	0.84	1.46	2.68	3.53	4.57
$n = 3$	1.05	1.77	3.00	4.02	4.67

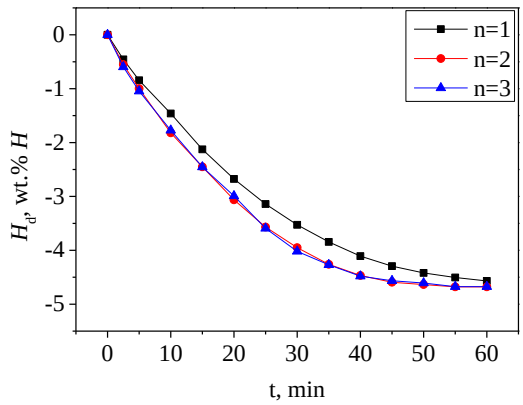

Fig. 4. Variation of the H_d vs. t curve of $90MgH_2$+5Ni+ +1.7$Zn(BH_4)_2$+1.7Ti+1.7Fe at 593 K under 1.0 bar H_2 with the number of cycles, n

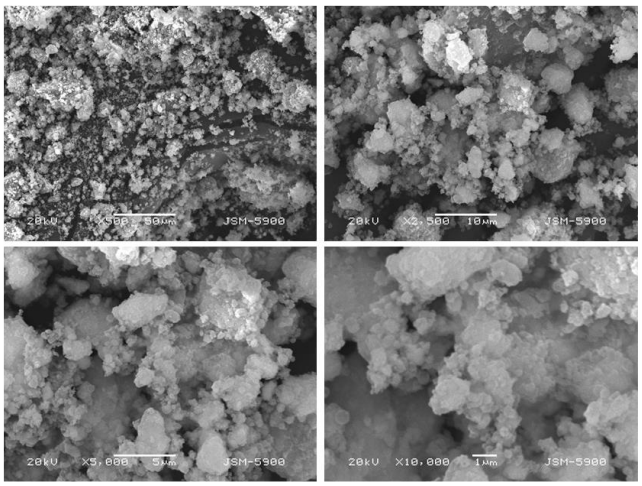

Fig. 5. SEM micrographs of $90MgH_2$+5Ni+1.7$Zn(BH_4)_2$+ +1.7 Ti+1.7Fe dehydrided at the 3rd hydriding-dehydriding cycle

The XRD pattern of $90MgH_2$+5Ni+1.7$Zn(BH_4)_2$+ +1.7Ti+1.7Fe dehydrided at the 3rd hydriding-dehydriding cycle is shown in Fig. 6. This sample has better crystallinity than the as-milled sample. The sample contains Mg and small amounts of β-MgH_2, MgO, Mg_2Ni, $TiH_{1.924}$, and Fe. This shows that Mg_2Ni formed from the

reaction of Ni with Mg, and $TiH_{1.924}$ formed by the reaction of Mg with hydrogen and is undecomposed even after dehydriding reaction.

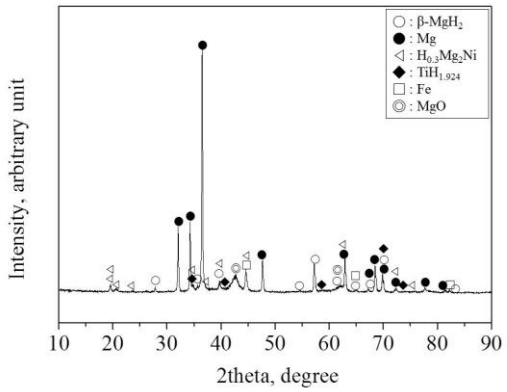

Fig. 6. XRD pattern of $90MgH_2$+5Ni+1.7Zn$(BH_4)_2$+1.7Ti+1.7Fe dehydrided at the 3rd hydriding-dehydriding cycle

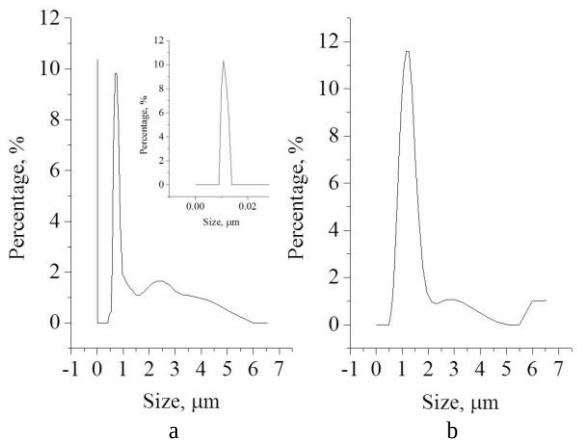

Fig. 7. Particle size distribution analysis results of $90MgH_2$+5Ni+1.7Zn$(BH_4)_2$+1.7Ti+1.7Fe (a) after milling in hydrogen and (b) after 3 hydriding-dehydriding cycles

Particle size distribution analysis results of $90MgH_2$+5Ni+1.7Zn$(BH_4)_2$+1.7Ti+1.7Fe after milling in hydrogen and after 3 hydriding-dehydriding cycles are shown in Fig. 7. The particle size distribution curves exhibit high peaks at about 0.01 and 0.7 μm for the sample after milling in hydrogen and a high peak at about 1.2 μm for the sample after 3 hydriding-dehydriding cycles. The sample after 3 hydriding-dehydriding cycles has larger particles than the sample after milling in hydrogen. The average particle size of the sample after milling in hydrogen was analyzed as 0.85 μm and that of the sample after 3 hydriding-dehydriding cycles was analyzed as 1.34 μm.

The BET plots of $90MgH_2$+5Ni+1.7Zn$(BH_4)_2$+ +1.7Ti+1.7Fe after milling in hydrogen and after 3 hydriding-dehydriding cycles are shown in Fig. 8. P and P_o are the equilibrium and the saturation pressure of adsorbates at the temperature of adsorption, and V_a is the adsorbed gas quantity (for example, in volume units). The BET specific surface area of the sample after milling in a hydrogen atmosphere is 57.9 m^2/g and that of the sample after 3 hydriding-dehydriding cycles is 53.2 m^2/g.

Fig. 9 shows the H_a vs. t curves under 12 bar H_2 at $n = 1$ for unmilled MgH_2 [30], unmilled Mg [31], and $90MgH_2$+5Ni+1.7Zn$(BH_4)_2$+1.7Ti+1.7Fe at 593 K and $94MgH_2$+6Ni [28] at 573 K. The $94MgH_2$ + 6Ni sample was prepared by milling in a hydrogen atmosphere under the conditions similar to those for the preparation of the $90MgH_2$+5Ni+1.7Zn$(BH_4)_2$+1.7Ti+1.7Fe sample.

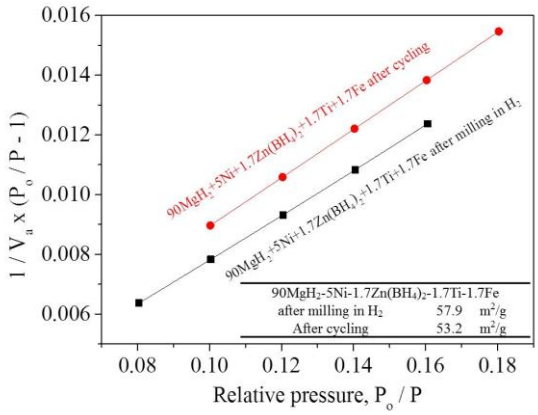

Fig. 8. BET plots of $90MgH_2$+5Ni+1.7Zn$(BH_4)_2$+1.7Ti+1.7Fe after milling in hydrogen and after 3 hydriding-dehydriding cycles

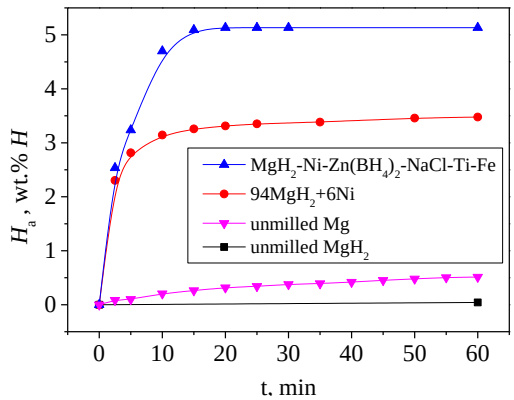

Fig. 9. H_a vs. t curves under 12 bar H_2 at $n = 1$ for unmilled MgH_2, unmilled Mg, and $90MgH_2$+5Ni+1.7Zn$(BH_4)_2$+ +1.7Ti+1.7Fe at 593 K and $94MgH_2$+6Ni at 573 K

Table 3. Variation of the absorbed hydrogen quantity with time under 12 bar H_2 at $n = 1$ for unmilled MgH_2, unmilled Mg, and $90MgH_2$+5Ni+1.7Zn$(BH_4)_2$+1.7Ti+1.7Fe at 593 K and $94MgH_2$ + 6Ni at 573 K

Absorbed hydrogen quantity (wt.% H)						
	2.5 min	5 min	10 min	15 min	25 min	60 min
Unmilled MgH_2	0					0.04
Unmilled Mg	0.09	0.10	0.20	0.26	0.34	0.51
$94MgH_2$+6Ni	2.30	2.81	3.14	3.26	3.35	3.48
$90MgH_2$+5Ni+ +1.7Zn$(BH_4)_2$+ +1.7Ti+1.7Fe		3.82	4.71	4.85		4.93

Unmilled MgH_2 absorbs hydrogen extremely slowly and unmilled Mg absorbs hydrogen slowly. $94MgH_2$+6Ni and $90MgH_2$+5Ni+1.7Zn$(BH_4)_2$+1.7Ti+1.7Fe have much higher initial hydriding rates and much larger quantities of hydrogen absorbed for 60 min than unmilled MgH_2 and unmilled Mg. $90MgH_2$+5Ni+1.7Zn$(BH_4)_2$+1.7Ti+1.7Fe has a larger initial hydriding rate and quantity of hydrogen absorbed for 60 min than $94MgH_2$ + 6Ni. Unmilled MgH_2

absorbs 0.04 wt.% H for 60 min. Unmilled Mg absorbs 0.20 wt.% H for 10 min and 0.51 wt.% H for 60 min. $94MgH_2$+6Ni absorbs 3.14 wt.% H for 10 min and 3.48 wt.% H for 60 min. $90MgH_2$+5Ni+1.7$Zn(BH_4)_2$+ +1.7Ti+1.7Fe absorbs 4.71 wt.% H for 10 min and 4.93 wt.% H for 60 min. Table 3 presents the variation of the absorbed hydrogen quantity with time for unmilled MgH_2, unmilled Mg, and $90MgH_2$+5Ni+ +1.7$Zn(BH_4)_2$+1.7Ti+1.7Fe at 593 K and $94MgH_2$ + 6Ni at 573 K under 12 bar H_2 at n = 1.

4. DISCUSSION

The XRD pattern of 78.3 wt.% $Zn(BH_4)_2$ + 21.7 wt.% MgH_2 after being heated up to 643 K showed that the sample contained NaCl, Zn, and MgH_2 [26]. NaCl was formed during synthesis of $Zn(BH_4)_2$ by milling $ZnCl_2$ and $NaBH_4$ [21]. This XRD pattern shows that Zn is formed by the decomposition of $Zn(BH_4)_2$ during heating. Nakagawa et al. [21] reported that $Zn(BH_4)_2$ releases hydrogen with toxic diborane (B_2H_6) after melting with increasing temperature. These indicate that $Zn(BH_4)_2$ decomposes into Zn, B_2H_6, and H_2 during heating.

For the measurements of hydriding and dehydriding properties, the sample was heated to 673 K and gases were released by pumping with a vacuum pump. It is thought that, during this time, NaCl, $TiH_{1.924}$, and Fe remain un-reacted, and the following reaction occurs:

$$Zn(BH_4)_2 + xMgH_2 + yNi \rightarrow Zn + B_2H_6 + yMg_2Ni + (x-2y)Mg + (x+1)H_2, \quad (1)$$

where x and y are stoichiometric coefficients.

During the subsequent hydriding-dehydriding cycling of $90MgH_2$+5Ni+1.7$Zn(BH_4)_2$+1.7Ti+1.7Fe, Zn, NaCl, $TiH_{1.924}$, and Fe remain un-reacted. Thus, during the subsequent hydriding-dehydriding cycling of this sample, the hydriding and dehydriding reactions of Mg and Mg_2Ni occur.

The SEM micrograph of Mg particles showed that the Mg particles are large and have smooth surfaces with a very small number of cracks [31]. The SEM micrographs of $90MgH_2$+5Ni+1.7$Zn(BH_4)_2$+1.7Ti+1.7Fe after milling in a hydrogen atmosphere, presented in Fig. 1, show that the particle size of the sample is not homogeneous and the sample has small particles, large particles, and agglomerates. Compared with Mg particles, $90MgH_2$+5Ni+1.7$Zn(BH_4)_2$+1.7Ti+1.7Fe particles have more defects and much smaller particle sizes. The BET specific surface area of the sample after milling in hydrogen was 57.9 m^2/g and that of the as-prepared $94MgH_2$+6Ni sample was 37.6 m^2/g [28]. This shows that addition of $Zn(BH_4)_2$, Ti, and Fe increases the BET specific surface area. The average particle sizes of unmilled MgH_2 [30], unmilled Mg [31], $94MgH_2$+6Ni [28], and $90MgH_2$+5Ni+1.7$Zn(BH_4)_2$+1.7Ti+1.7Fe were 0.65, 0.25, 0.83, and 0.85 μm. $90MgH_2$+5Ni+1.7$Zn(BH_4)_2$+ +1.7Ti+1.7Fe does not have the smallest average particle size, but it has the highest initial hydriding rate and the largest value of H_a(60 min). The initial hydriding rate and the value of H_a(60 min) are not proportional to the decrease in the average particle size of the sample. This means that, in addition to the average particle size, other factors such as number of defects and cleanness of the particle surfaces determine the initial hydriding rate and the value of H_a(60 min). The milling in a hydrogen atmosphere of MgH_2 with Ni, $Zn(BH_4)_2$, Fe, and Ti is thus believed to increase the hydriding and dehydriding rates by producing defects [32 – 34] on the surface and in the inside of particles, generating newly exposed clean surfaces [34, 35], and decrease the particle size of MgH_2 [32, 35 – 38]. The production of defects facilitates nucleation, generating newly exposed clean surfaces improves the reactivity of surfaces, and the decrease of the particle size reduces the diffusion distances of hydrogen atoms [39 – 41]. These effects are believed to increase the hydriding and dehydriding rates of MgH_2.

Mg_2Ni has much higher hydriding and dehydriding rates than Mg at about 573 K [27]. The Mg_2Ni phase formed after hydriding-dehydriding cycling is also believed to increase the hydriding and dehydriding rates of MgH_2.

$TiH_{1.924}$, Fe, Zn, NaCl, and MgO, remaining un-reacted during hydriding-dehydriding cycling, are believed to prevent the particles from being coalesced during hydriding-dehydriding cycling.

$90MgH_2$+5Ni+1.7$Zn(BH_4)_2$+1.7Ti+1.7Fe has an effective hydrogen-storage capacity (the quantity of hydrogen absorbed for 60 min) of 5 wt.%.

In the sample after 3 hydriding-dehydriding cycles, particles are larger (Fig. 5), has a larger average particle size (Fig. 7), and has a smaller BET specific surface area (Fig. 8), compared with those in the sample after milling in hydrogen. It is believed that particles become larger due to coalescence of particles because hydriding-dehydriding cycling was performed at a relatively high temperature of 593 K.

5. CONCLUSIONS

90wt.%MgH_2+5wt.%Ni+1.7wt.% $Zn(BH_4)_2$+ 1.7 wt.% Ti+1.7wt.%Fe samples (named $90MgH_2$+5Ni+ +1.7$Zn(BH_4)_2$+1.7Ti+1.7Fe) were prepared by milling in a planetary ball mill in a hydrogen atmosphere. $90MgH_2$+5Ni+1.7$Zn(BH_4)_2$+1.7Ti+1.7Fe had an effective hydrogen storage capacity of 5 wt.%. The activation of the sample was completed after 2 hydriding-dehydriding cycles. The as-milled $90MgH_2$+5Ni+1.7$Zn(BH_4)_2$+ +1.7Ti+1.7Fe sample contained β-MgH_2, γ-MgH_2, Ni, Ti, Fe, and MgO. The sample dehydrided at the 3rd hydriding-dehydriding cycle contained Mg and small amounts of β-MgH_2, MgO, Mg_2Ni, $TiH_{1.924}$, and Fe. The BET specific surface area of the sample after milling in hydrogen was 57.9 m^2/g and that of the sample after 3 hydriding-dehydriding cycles was 53.2 m^2/g. At n = 3, the sample absorbed 4.14 wt.% H for 5 min and 5.00 wt.% H for 60 min at 593 K under 12 bar H_2. At n = 3, the sample desorbed 1.77 wt.% H for 10 min and 4.67 wt.% H for 60 min at 593 K under 1.0 bar H_2. The milling in a hydrogen atmosphere of MgH_2 with Ni, $Zn(BH_4)_2$, Ti, and Fe is believed to facilitate nucleation, improve the reactivity of surfaces, and reduce the diffusion distances of hydrogen atoms.

Acknowledgments

This research was supported by a grant (2013 Ha A17) from Jeonbuk Research & Development Program funded by Jeonbuk Province.

REFERENCES

1. **Han, J.S., Kim, S.J., Kim, D.I.** A Study of the Pressure-Composition-Temperature Curve of $Mg(BH_4)_2$ by Sievert`s Type Apparatus *Korean Journal of Metals and Materials* 53 2015: pp. 815 – 820.
2. **Lee, S.H., Kwak, Y.J., Park, H.R., Song, M.Y.** Enhancement of the Hydriding and Dehydriding Rates of Mg by Adding $TiCl_3$ and Reactive Mechanical Grinding *Korean Journal of Metals and Materials* 53 2015: pp. 187 – 192.
3. **Hong, S.H., Song, M.Y.** Preparation of a Single MgH_2 Phase by Horizontal Ball Milling and the First Hydriding Reaction of 90 wt% Mg-10 wt% MgH_2 *Metals and Materials International* 21 2015: pp. 422 – 428. https://doi.org/10.1007/s12540-015-4288-y
4. **Song, M.Y, Kwak, Y.J., Lee, S.H., Park, H.R.** Hydriding and Dehydriding Rates of Mg, Mg-10TaF_5, and Mg-10NbF_5 Prepared via Reactive Mechanical Grinding *Metals and Materials International* 21 2015: pp. 208 – 212. https://doi.org/10.1007/s12540-015-1027-3
5. **Mumm, D.R., Kwak, Y.J., Park, H.R., Song, M.Y.** Effects of Milling and Hydriding-Dehydriding Cycling on the Hydrogen-Storage Behaviors of a Magnesium-Nickel-Tantalum Fluoride Alloy *Korean Journal of Metals and Materials* 53 2015: pp. 904 – 910.
6. **Lee, S.H., Park, H.R., Song, M.Y.** Change in Hydrogen-Storage Performance of Transition Metals and $NaAlH_4$–Added MgH_2 with Thermal and Hydriding-Dehydriding Cycling *Korean Journal of Metals and Materials* 53 2015: pp. 133 – 138.
7. **Mumm, D.R., Lee, S.H., Song, M.Y.** Cycling Behavior of Transition Metals and Sodium Alanate-Added MgH_2 Kept in a Glove Box *Korean Journal of Metals and Materials* 53 2015: pp. 584 – 590.
8. **Bobet, J.L., Akiba, E., Darriet, B.** Study of Mg-M (M=Co, Ni and Fe) Mixture Elaborated by Reactive Mechanical Alloying: Hydrogen Sorption Properties *International Journal of Hydrogen Energy* 26 2001: pp. 493 – 501. https://doi.org/10.1016/S0360-3199(00)00082-3
9. **Li, Z., Liu, X., Jiang, L., Wang, S.** Characterization of Mg–20 wt% Ni–Y Hydrogen Storage Composite Prepared by Reactive Mechanical Alloying *International Journal of Hydrogen Energy* 32 2007: pp. 1869 – 1874.
10. **Boulet, J.M. Gerard, N.** The Mechanism and Kinetics of Hydride Formation in Mg-10 wt% Ni and $CeMg_{12}$ *Journal of the Less-Common Metals* 89 1983: pp. 151 – 161. https://doi.org/10.1016/0022-5088(83)90261-8
11. **Züttel, A., Rentsch, S., Fisher, P., Wenger, P., Sudan, P., Mauron, Ph., Emmenegger, Ch.** Hydrogen Storage Properties of $LiBH_4$ *Journal of Alloys and Compounds* 356 – 357 2003: pp. 515 – 520.
12. **Orimo, S., Nakamori, Y., Züttel, A.** Material Properties of MBH_4 (M=Li, Na, and K) *Materials Science and Engineering: B* 108 2004: pp. 51 – 53. https://doi.org/10.1016/j.mseb.2003.10.045
13. **Hagemann, H., Gomes, S., Renaudin, G., Yvon, K.** Raman Studies of Reorientation Motions of $[BH_4]^-$ Anionsin Alkali Borohydrides *Journal of Alloys and Compounds* 363 2004: pp. 129 – 132. https://doi.org/10.1016/S0925-8388(03)00468-7
14. **Renaudin, G., Gomes, S., Hagemann, H., Keller, L., Yvon, K.** Structural and Spectroscopic Studies on the Alkali Borohydrides MBH_4 (M = Na, K, Rb, Cs) *Journal of Alloys and Compounds* 375 2004: pp. 98 – 106. https://doi.org/10.1016/j.jallcom.2003.11.018
15. **Yoshino, M., Komiya, K., Takahashi, Y., Shinzato, Y., Yukawa, H., Morinaga, M.** Nature of the Chemical Bond in Complex Hydrides, $NaAlH_4$, $LiAlH_4$, $LiBH_4$ and $LiNH_2$ *Journal of Alloys and Compounds* 404 – 406 2005: pp. 185-190.
16. **Orimo, S., Nakamori, Y., Kitahara, G., Miwa, K., Ohba, N., Towata, S., Züttel, A.** Dehydriding and Rehydriding Reactions of $LiBH_4$ *Journal of Alloys and Compounds* 404 – 406 2005: pp. 427 – 430.
17. **Kang, J.K., Kim, S.Y., Han, Y.S., Muller, R.P., Goddard, W.A.** A Candidate $LiBH_4$ for Hydrogen Storage: Crystal Structures and Reaction Mechanisms of Intermediate Phases *Applied Physics Letters* 87 2005: pp. 111904 – 111904-3.
18. **Kumar, R.S., Cornelius, A.L.** Structural Transitions in $NaBH_4$ under Pressure *Applied Physics Letters* 87 2005: pp. 261916 – 261916-3.
19. **Nakamori, Y., Miwa, K., Ninomiya, A., Li, H.W., Ohba, N., Towata, S., Züttel, A., Orimo, S.** Correlation between Thermodynamical Stabilities of Metal Borohydrides and Cation Electronegativites: First-Principles Calculations and Experiments *Physical Review B* 74 2006: pp. 045126.
20. **Nakamori, Y., Li, H.W., Miwa, K., Towata, S., Orimo, S.** Syntheses and Hydrogen Desorption Properties of Metal-Borohydrides $M(BH_4)_n$ (M= Mg, Sc, Zr, Ti, and Zn; n=2-4) as Advanced Hydrogen Storage Materials *Materials Transactions* 47 (8) 2006: pp. 1898 – 1901.
21. **Nakagawa, T., Ichikawa, T., Kojima, Y., Fujii, H.** Gas Emission Properties of the MgH_x-$Zn(BH_4)_2$ Systems *Materials Transactions* 48 (3) 2007: pp. 556 – 559. https://doi.org/10.2320/matertrans.48.556
22. **Setamdideh, D., Khaledi, L.** $Zn(BH_4)_2$/2NaCl: A Novel Reducing System for Efficient Reduction of Organic Carbonyl Compounds to Their Corresponding Alcohols *South African Journal of Chemistry* 66 2013: pp. 150 – 157.
23. **Jeon, E., Cho, Y.W.** Mechanochemical Synthesis and Thermal Decomposition of Zinc Borohydride *Journal of Alloys and Compounds* 422 2006: pp. 273 – 275.
24. **Jeon, E., Cho, Y.W.** Synthesis and Thermal Decomposition of $Zn(BH_4)_2$ *Transactions of the Korean Hydrogen and New Energy Society* 16 2005: pp. 262 – 268.
25. **Shahi, R.R., Tiwari, A.P., Shaz, M.A., Srivastava, O.N.** Studies on De/Rehydrogenation Characteristics of Nanocrystalline MgH_2 Co-Catalyzed with Ti, Fe and Ni *International Journal of Hydrogen Energy* 6 2013: pp. 2778 – 2784. https://doi.org/10.1016/j.ijhydene.2012.11.073
26. **Kwak, Y.J., Kwon, S.N., Song, M.Y.** Preparation of $Zn(BH_4)_2$ and Diborane and Hydrogen Release Properties of $Zn(BH_4)_2$+xMgH_2 (x=1, 5, 10, and 15) *Metals and Materials International* 21 2015: pp. 971 – 976. https://doi.org/10.1007/s12540-015-4604-6
27. **Akiba, E., Nomura, K., Ono, S., Suda, S.** Kinetics of the reaction between Mg-Ni alloys and H_2 *International Journal of Hydrogen Energy* 7 1982: pp. 787 – 791. https://doi.org/10.1016/0360-3199(82)90069-6

28. **Kwak, Y.J., Lee, S.H., Park, H.R., Song, M.Y.** Hydrogen-Storage Property Enhancement of Magnesium Hydride by Nickel Addition via Reactive Mechanical Grinding *Korean Journal of Metals and Materials* 51 2013: pp. 607 – 613.

29. **Song, M.Y., Baek Bobet, J.L., Song, J., Hong, S.H.** Hydrogen Storage Properties of a Mg–Ni–Fe Mixture Prepared via Planetary Ball Milling in a H_2 Atmosphere *International Journal of Hydrogen Energy* 35 2010: pp. 10366 – 10372. https://doi.org/10.1016/j.ijhydene.2010.07.161

30. **Song, M.Y., Kwak, Y.J., Lee, S.H., Park, H.R.** Comparison of Hydrogen Storage Properties of Pure MgH_2 and Pure Mg *Korean Journal of Metals and Materials* 52 2014: pp. 689 – 693.

31. **Song, M.Y., Kwak, Y.J., Lee, S.H., Park, H.R.** Comparison of the Hydrogen Storage Properties of Pure Mg and Milled Pure Mg *Bulletin of Materials Science* 37 2014: pp. 831 – 835.

32. **Song, M.Y., Ivanov, E.I., Darriet, B., Pezat, M., Hagenmuller, P.** Hydriding and Dehydriding Characteristics of Mechanically Alloyed Mixtures Mg-xwt.%Ni (x = 5, 10, 25, and 55) *Journal of the Less-Common Metals* 131 1987: pp. 71 – 79. https://doi.org/10.1016/0022-5088(87)90502-9

33. **Vigeholm, B., Kjoller, J., Larsen, B., Pedersen, A.S.** Formation and Decomposition of Magnesium Hydride *Journal of the Less-Common Metals* 89 1983: pp. 135 – 144. https://doi.org/10.1016/0022-5088(83)90259-X

34. **Jain, I.P., Lal, C., Jain, A.** Hydrogen Storage in Mg: A Most Promising Material *International Journal of Hydrogen Energy* 35 2010: pp. 5133 – 5144. https://doi.org/10.1016/j.ijhydene.2009.08.088

35. **David, E.** Nanocrystalline Magnesium and its Properties of Hydrogen Sorption *Journal of Achievements in Materials and Manufacturing Engineering* 20 2007: pp. 87 – 90.

36. **Spassov, T., Delchev, P., Madjarov, P., Spassova, M., Himitliiska, T.** Hydrogen Storage in Mg–10 at.% $LaNi_5$ Nanocomposites, Synthesized by Ball Milling at Different Conditions *Journal of Alloys and Compounds* 495 2010: pp. 149 – 153.

37. **Zaluska, A., Zaluski, L., Ström-Olsen, J.O.** Nanocrystalline Magnesium for Hydrogen Storage *Journal of Alloys and Compounds* 288 1999: pp. 217 – 225.

38. **Aguey-Zinsou, K.F., Ares Fernandez, J.R., Klassen, T., Bormann, R.** Using MgO to Improve the (De)Hydriding properties of magnesium *Materials Reearch Bulletin* 41 2006: pp. 1118 – 1126.

39. **Hong, S.H., Song, M.Y.** MgH_2 and Ni-Coated Carbon-Added Mg Hydrogen-Storage Alloy Prepared by Mechanical Alloying *Korean Journal of Metals and Materials* 54 2016: pp. 125 – 131.

40. **Hong, S.H., Song, M.Y.** Study on the Reactivity with Hydrogen of Planetary Ball Milled 90 wt.% Mg + 10 wt.% MgH_2: Analyses of Reaction Rates with Hydrogen and Microstructure *Korean Journal of Metals and Materials* 54 2016: pp. 358 – 363.

41. **Kwak, Y.J., Kwon, S.N., Song, M.Y.** Hydriding and Dehydriding properties of Zinc Borohydride, Nickel, and Titanium-Added Magnesium Hydride *Korean Journal of Metals and Materials* 53 2015:pp. 808 – 814.